Coordination Chemistry Reviews
175 (1998) 59–89

Ruthenium cluster–[2.2]paracyclophane complexes

Paul J. Dyson [a,*], Brian F.G. Johnson [b], Caroline M. Martin [b]

[a] Centre for Chemical Synthesis, Department of Chemistry, Imperial College of Science, Technology and Medicine, South Kensington, London SW7 2AY, UK
[b] University Chemical Laboratories, Lensfield Road, Cambridge CB2 1EW, UK

Received 19 February 1998; accepted 19 June 1998

Contents

---

[*] Corresponding author. Tel.: +44-1904-434076; e-mail: pjd14@york.ac.uk

PII S0010-8545(98)00172-6

Abstract

The last few years have seen a rapid expansion in the synthesis and characterisation of cluster–arene complexes. One arene ligand which has been found to be particularly versatile in cluster chemistry is [2.2]paracyclophane. In this article we review the chemistry of [2.2]paracyclophane clusters with regard to their synthesis, reactivity and structure.

Keywords: Ruthenium; Clusters; [2.2]Paracyclophane

1. Introduction

In 1949, Brown and Farthing reported the isolation of di-*p*-xylene from the high-temperature pyrolysis (900 °C) of *p*-xylene [1]. Since it was not possible at that time to prepare the compound by a more conventional route, it was concluded that the ring-strain evidently present in the molecule could only be overcome by the extreme conditions of the pyrolysis reaction. These initial inferences were proved incorrect just two years later by Cram and Steinberg who, whilst looking at the bonding, strain energies and transannular π-electron interactions within rigid molecules of known geometry, prepared di-*p*-xylene by design via the intramolecular Würtz-coupling reaction of dibromo-*p*-xylene [2]. Cram and Steinberg introduced the cyclophane nomenclature which was later reinforced by Vögtle and is now commonly used for this class of compounds [3]. The term ‘cyclophane’ describes any molecule containing a bridged aromatic ring, and each bridge is indicated by a number (corresponding to the number of bridge members) placed in a bracket before the name [4]. According to this nomenclature, di-*p*-xylene can be referred to as [2.2]paracyclophane or [2.2](1,4)cyclophane. A number of cyclophane molecules were known under a variety of different names many years before this period: for example, [2.2]metacyclophane was first observed in 1899 [5]. However, Cram laid the basis for the synthesis of a whole new group of aromatic compounds. He also outlined many of the reasons why cyclophane chemistry has become an exciting area of research.

Cyclophane molecules which contain benzene exhibit cofacial π–π repulsions that result in the distortion of the benzene ring from planarity towards either boat or chair conformations. As a result, they provide excellent models for the study of molecular strain and its relationship to reactivity. The conformational simplicity and unique geometry of these cyclophane molecules also provide a means of investigating the transannular steric and electronic interactions between the aromatic rings, and therefore allows the question of whether and how the electronic effects of substituents in one ring are transferred to the second ring and how these interactions vary with the bridge length.

A large number of cyclophane molecules have been prepared [6], in which many types of aromatic subunits are bridged. They are bridged not only by polymethylene chains, but also by functionalised bridging units. Much of the early work centred around the $[2_n]$cyclophanes (aromatic compounds containing two benzene rings connected by n ethano bridges) and by 1980 all 12 of the 'symmetrical' $[2_n]$cyclophanes (i.e. those in which the bridges are aligned in parallel and anchored to identical positions of both aromatic nuclei) had been prepared (Fig. 1).

The first transition-metal complex of paracyclophane, i.e. $Cr(CO)_3(\eta^6\text{-}C_{16}H_{16})$ [7], was prepared in 1960 and in 1978 its structure was established by single-crystal X-ray analysis [8]. Upon complexation the topology of the cyclophane unit is significantly altered due to the electron withdrawing effect of the $Cr(CO)_3$ group, which reduces the inherent strain of the molecule. The initial work on chromium–cyclophane complexes demonstrated the potential that this class of compounds could offer as π-ligands in organometallic chemistry. A large number of cyclophane–metal complexes are now known and there are examples involving Cr, Mo, W, Fe, Ru, Os, Co, Rh, Ir, Ni, Cu, Ag and U metals. These complexes are not only based on the six-membered ring system phanes, but also rings with four, five, seven and eight carbon atoms. Several reviews have recently appeared which deal with the organometallic chemistry of cyclophanes [9–11].

We have been interested in the synthesis and characterisation of cluster–arene complexes for a number of years [12], and some recent work has been concerned with the interaction of ruthenium clusters with the [2.2]paracyclophane ligand. This

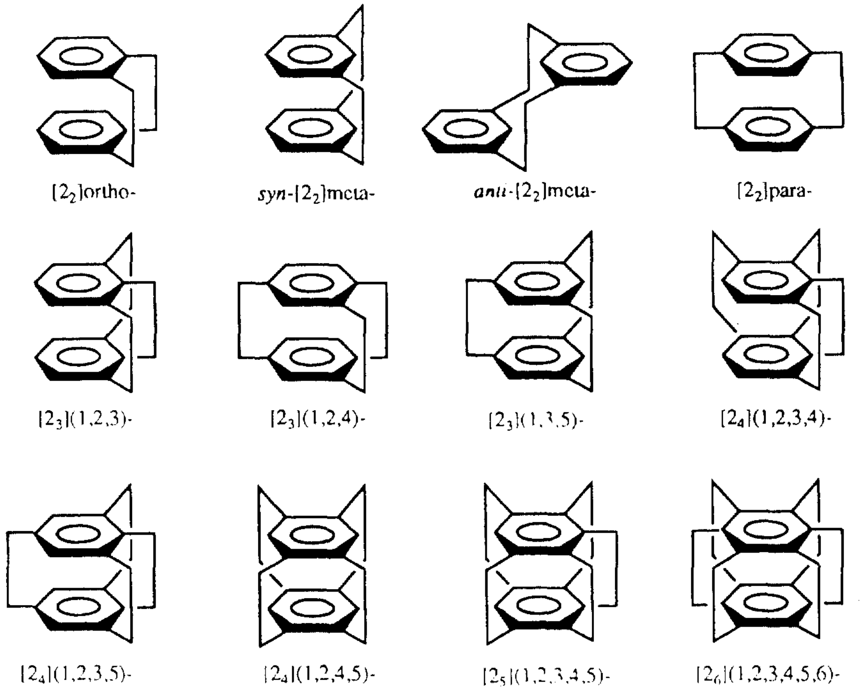

$[2_2]$ortho-, *syn*-$[2_2]$meta-, *anti*-$[2_2]$meta-, $[2_2]$para-

$[2_3]$(1,2,3)-, $[2_3]$(1,2,4)-, $[2_3]$(1,3,5)-, $[2_4]$(1,2,3,4)-

$[2_4]$(1,2,3,5)-, $[2_4]$(1,2,4,5)-, $[2_5]$(1,2,3,4,5)-, $[2_6]$(1,2,3,4,5,6)-

Fig. 1. The 'symmetrical' $[2_n]$cyclophanes.

ligand, which may interact with one or more metal atoms, also mediates cluster build-up, and some unusual cluster polyhedra have been produced. We describe these studies and compare the results, where appropriate, to mononuclear complexes.

2. Synthesis

2.1. Clusters obtained from the direct reaction between $Ru_3(CO)_{12}$ and [2.2]paracyclophane

The reaction between $Ru_3(CO)_{12}$ and [2.2]paracyclophane in octane, under reflux, affords a range of products with nuclearities ranging from three to eight [13–17]. These products have been characterised as $Ru_3(CO)_9(\mu_3\text{-}C_{16}H_{16})$ [13], $Ru_6C(CO)_{15}(\mu_3\text{-}C_{16}H_{16}\text{-}\mu_2\text{-}O)$ [14], $Ru_6C(CO)_{14}(\mu_3\text{-}C_{16}H_{16})$ [15], $Ru_6C(CO)_{11}(\mu_3\text{-}C_{16}H_{16})(\eta^6\text{-}C_{16}H_{16})$ [16] and $Ru_8(\mu\text{-}H)_4(CO)_{18}(\eta^6\text{-}C_{16}H_{16})$ [17] (Scheme 1). The distribution of these products can be optimised by careful control of the reaction time. A reaction period of 1 h gives mostly the trinuclear derivative, $Ru_3(CO)_9(\mu_3\text{-}C_{16}H_{16})$, whereas 3 h yields mostly the hexanuclear cluster, $Ru_6C(CO)_{14}(\mu_3\text{-}C_{16}H_{16})$, and as the time is increased beyond 3 h, larger quantities of $Ru_6C(CO)_{11}(\mu_3\text{-}C_{16}H_{16})(\eta^6\text{-}C_{16}H_{16})$ and $Ru_8(\mu\text{-}H)_4(CO)_{18}(\eta^6\text{-}C_{16}H_{16})$ are obtained. When the analogous reaction is carried out in heptane a similar range of products are isolated, with enhanced yields of $Ru_3(CO)_9(\mu_3\text{-}C_{16}H_{16})$ and $Ru_6C(CO)_{15}(\mu_3\text{-}C_{16}H_{16}\text{-}\mu_2\text{-}O)$, and two additional octaruthenium products, not observed in the octane reaction, are isolated in low yield. These two compounds have been characterised by X-ray crystallography as $Ru_8(\mu\text{-}H)_2(\mu_6\text{-}\eta^2\text{-}CO)(CO)_{19}(\eta^6\text{-}C_{16}H_{16})$ and $Ru_8(\mu_6\text{-}\eta^2\text{-}CO)(\mu_4\text{-}\eta^2\text{-}CO)(CO)_{18}(\eta^6\text{-}C_{16}H_{16})$ [18].

It is not fully understood why such a wide range of cyclophane clusters are produced from these thermal reactions. Under conditions of moderately high temperatures, conversion of $Ru_3(CO)_{12}$ to $Ru_6C(CO)_{17}$ is known to occur, producing an alternative reaction pathway to Ru_6C based derivatives. However, these reactions are clearly more complicated and cannot be understood from this alone. In related studies involving the thermolysis of $Ru_3(CO)_{12}$ and mesitylene in octane or heptane three neutral hexaruthenium mesitylene clusters have been isolated, these being $Ru_6(\eta^2\text{-}\mu_4\text{-}CO)_2(CO)_{13}(\eta^6\text{-}C_6H_3Me_3)$, $HRu_6(\eta^2\text{-}\mu_4\text{-}CO)(CO)_{13}(\mu_2\text{-}\eta^1\text{:}\eta^6\text{-}C_6H_3Me_2CH_2)$ and $Ru_6C(CO)_{14}(\eta^6\text{-}C_6H_3Me_3)$ [19]. In other arene systems, only the *closo*-octahedral carbido clusters, $Ru_6C(CO)_{14}(\eta^6\text{-arene})$ (arene = C_6H_6, C_6H_5Me and $C_6H_4Me_2$), have been isolated together with the parent cluster, $Ru_6C(CO)_{17}$ [20]. With [2.2]paracyclophane the relatively large number of clusters obtained may arise from a mechanism involving both its rings. It is possible that incoming metal fragments may attach to one ring and then transfer to the other such that cluster growth may occur by more than one mechanism. This could give rise to the diversity found within this reaction, although no direct evidence has been obtained in support of this suggestion. In initial studies, it was hoped that [2.2]paracyclophane would act as a bridging ligand, with a cluster unit attached to

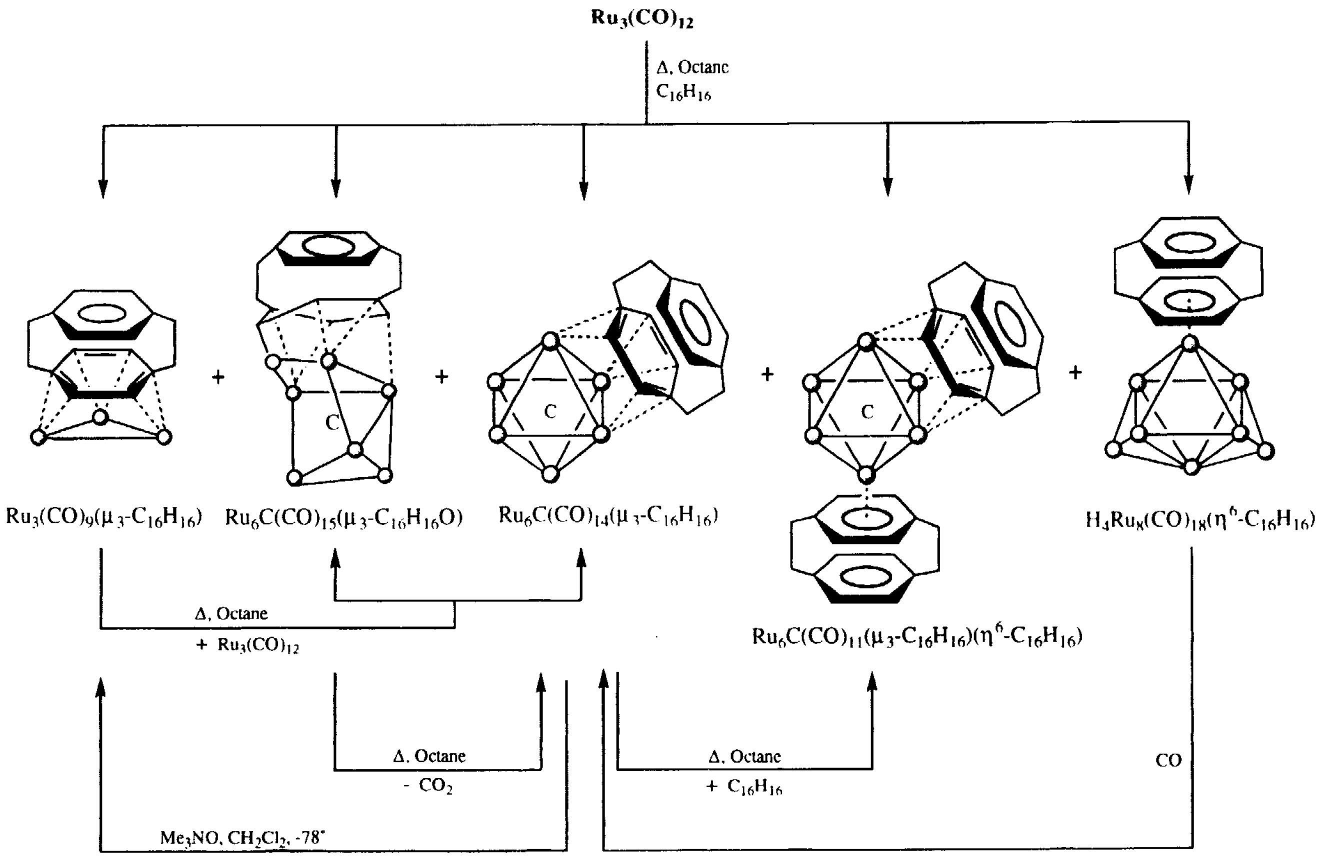

Scheme 1. The reaction of $Ru_3(CO)_{12}$ with [2.2]paracyclophane. Carbonyl ligands are omitted for clarity.

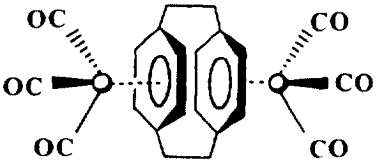

Fig. 2. $\{Cr(CO)_3\}_2(\eta^6\text{-}\eta^6\text{-}C_{16}H_{16})$.

either ring in an analogous fashion to the bis(chromium) complex, $\{Cr(CO)_3\}_2(\eta^6\text{-}\eta^6\text{-}C_{16}H_{16})$ (Fig. 2) [21]. However, no species of this type has, as yet, been identified from conventional preparative methods. This is not totally unexpected since the coordination of a cluster to one of the rings in [2.2]paracyclophane results in deactivation of the other ring towards further coordination. Thus, any such bridging species produced is expected to be highly unstable and undergo further chemical transformations.

It is also noteworthy that higher yields are obtained in the reactions employing [2.2]paracyclophane as opposed to other simple arenes. This is because [2.2]paracyclophane is a stronger nucleophile than simple arenes as π-electron density is pushed towards the outer faces of the rings due to their close proximity.

2.2. Interconversion of the [2.2]paracyclophane clusters: relevance to carbide formation

The relationships between the clusters produced from the thermal reaction between $Ru_3(CO)_{12}$ and [2.2]paracyclophane has emerged. On heating $Ru_3(CO)_9(\mu_3\text{-}C_{16}H_{16})$ in octane with an equimolar quantity of $Ru_3(CO)_{12}$, both $Ru_6C(CO)_{15}(\mu_3\text{-}C_{16}H_{16}\text{-}\mu_2\text{-}O)$ and $Ru_6C(CO)_{14}(\mu_3\text{-}C_{16}H_{16})$ are produced [14]. Furthermore, the thermolysis of $Ru_6C(CO)_{15}(\mu_3\text{-}C_{16}H_{16}\text{-}\mu_2\text{-}O)$ in octane or its pyrolysis in a gas cell yields $Ru_6C(CO)_{14}(\mu_3\text{-}C_{16}H_{16})$ and CO_2 in near quantitative yields. Clearly, $Ru_6C(CO)_{15}(\mu_3\text{-}C_{16}H_{16}\text{-}\mu_2\text{-}O)$ is an intermediate on route to the carbido cluster $Ru_6C(CO)_{14}(\mu_3\text{-}C_{16}H_{16})$, requiring the loss of CO_2 and a rearrangement of the ruthenium atom skeleton (Scheme 2).

Carbide formation has also been observed in the mesitylene cluster, $Ru_6(\eta^2\text{-}\mu_4\text{-}CO)_2(CO)_{13}(\eta^6\text{-}C_6H_3Me_3)$ [19], which has a metal framework defined by a tetrahedral Ru_4 arrangement with two additional edge-bridging ruthenium atoms. Thermolysis of this cluster in mesitylene results in conversion to the *closo*-cluster, $Ru_6C(CO)_{14}(\eta^6\text{-}C_6H_3Me_3)$, with concomitant evolution of CO_2.

Thermolysis of $Ru_6C(CO)_{14}(\mu_3\text{-}C_{16}H_{16})$ with an excess of [2.2]paracyclophane in octane yields $Ru_6C(CO)_{11}(\eta^6\text{-}C_{16}H_{16})(\mu_3\text{-}C_{16}H_{16})$ in which three carbonyl ligands have been displaced by the second paracyclophane moiety. It is also possible to convert $Ru_6C(CO)_{14}(\mu_3\text{-}C_{16}H_{16})$ back to $Ru_3(CO)_9(\mu_3\text{-}C_{16}H_{16})$ by degradation of the

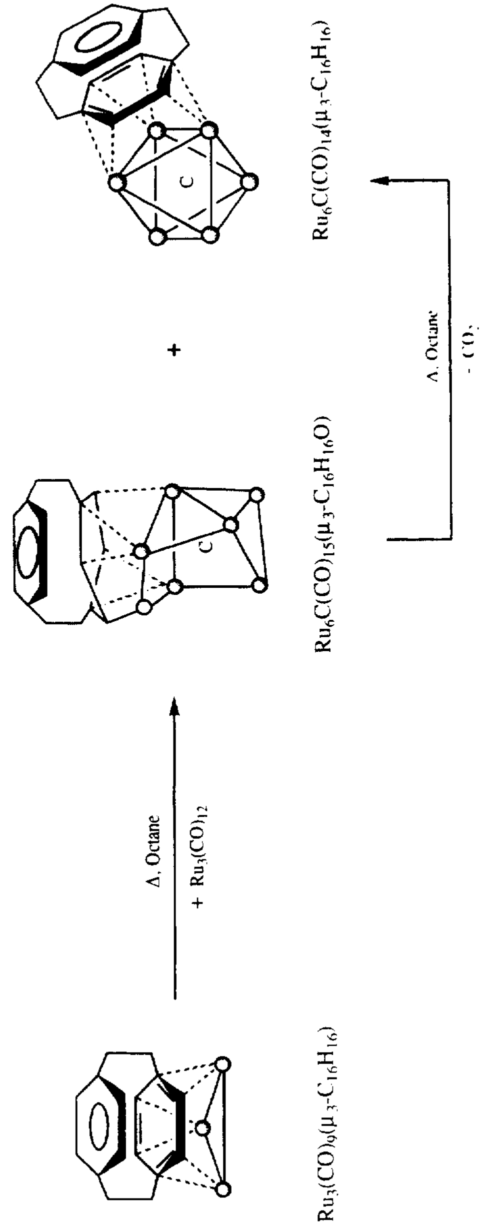

Scheme 2. The formation of $Ru_6C(CO)_{14}(\mu_3\text{-}C_{16}H_{16})$.

cluster core using a large excess of the oxidative decarbonylation reagent trimethylamine *N*-oxide in a coordinatively inert solvent such as dichloromethane [13].

In a highly unusual reaction, the octaruthenium cluster, $Ru_8(\mu\text{-}H)_4(CO)_{18}(\eta^6\text{-}C_{16}H_{16})$, reacts with CO in dichloromethane at room temperature to give $Ru_3(CO)_{12}$ and $Ru_6C(CO)_{14}(\mu_3\text{-}C_{16}H_{16})$ [17]. Whilst it is easy to envisage that the $Ru_3(CO)_{12}$ produced in this reaction is derived from a recombination of ruthenium carbonyl fragments generated from the carbonylation of the capping groups on the starting material, the formation of the carbido cluster, $Ru_6C(CO)_{14}(\mu_3\text{-}C_{16}H_{16})$, is less easy to envisage as the entrapment of a carbido atom into the preformed octahedral cavity is necessary.

Although there is no direct evidence, it is possible that $Ru_8(\mu\text{-}H)_2(\mu_6\text{-}\eta^2\text{-}CO)(CO)_{19}(\eta^6\text{-}C_{16}H_{16})$ and $Ru_8(\mu_6\text{-}\eta^2\text{-}CO)(\mu_4\text{-}\eta^2\text{-}CO)(CO)_{18}(\eta^6\text{-}C_{16}H_{16})$ with their open metal framework and elongated *dihapto* carbonyl ligand may represent the type of intermediate formed during this process (Scheme 3) [18]. For example, from an inspection of the molecular structure of $Ru_8(\mu\text{-}H)_2(\mu_6\text{-}\eta^2\text{-}CO)(CO)_{19}(\eta^6\text{-}C_{16}H_{16})$ (see below) we may speculate that cleavage of the activated *dihapto* C–O bond (by loss of the O atom as CO_2) would cause the resulting carbide atom to be pulled up into the plane of the four ruthenium atoms to which it is attached, resulting in a movement of the ruthenium atoms to form an octahedron. Clearly two ruthenium atoms must be cleaved [which may then undergo recombination to form $Ru_3(CO)_{12}$ in the presence of excess CO]. The formation of several Ru–Ru bonds is also required for the generation of a *closo*-octahedron, but this is not unexpected if the cluster would otherwise be coordinatively unsaturated.

2.3. *The reaction of $Ru_4(CO)_{12}(\mu_4\text{-}C_6H_8)$ with [2.2]paracyclophane*

Thermolysis of the butterfly cluster $Ru_4(CO)_{12}(\mu_4\text{-}C_6H_8)$ with [2.2]paracyclophane in octane affords two cluster isomers, $Ru_4(CO)_9(\mu_4\text{-}C_6H_8)(\eta^6\text{-}C_{16}H_{16})$ and $Ru_4(CO)_9(\mu_4\text{-}C_6H_8)(\mu_3\text{-}C_{16}H_{16})$ (Scheme 4) [22]. The addition of three molecular equivalents of Me_3NO to the reaction mixture during the reflux increases the yield of both the products. $Ru_4(CO)_9(\mu_4\text{-}C_6H_8)(\eta^6\text{-}C_{16}H_{16})$ slowly isomerises to $Ru_4(CO)_9(\mu_4\text{-}C_6H_8)(\mu_3\text{-}C_{16}H_{16})$ on standing at room temperature, alternatively it can be converted quantitatively by heating in dichloromethane for several hours. The migration of [2.2]paracyclophane from one coordination site to another will be described in more detail in Section 3.6.

3. Reactivity

3.1. *General reactivity of [2ₙ]cyclophanes*

The way in which a substituent on one ring of [2.2]paracyclophane has a directing influence for electrophilic substitution in the second ring was of primary interest shortly after cyclophanes were first recognised [23]. These transannular substituent effects, as they are now known, are summarised by the reaction shown

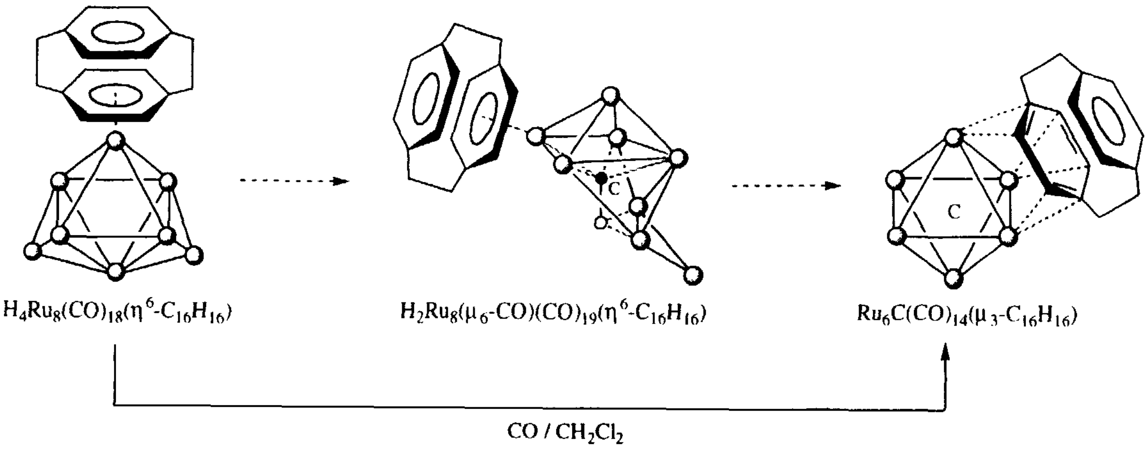

Scheme 3. The conversion of $Ru_8(\mu-H)_4(CO)_{18}(\eta^6-C_{16}H_{16})$ into $Ru_6C(CO)_{14}(\mu_3-C_{16}H_{16})$, showing $Ru_8(\mu-H)_2(\mu_6-\eta^2-CO)(CO)_{19}(\eta^6-C_{16}H_{16})$ as a possible reaction intermediate.

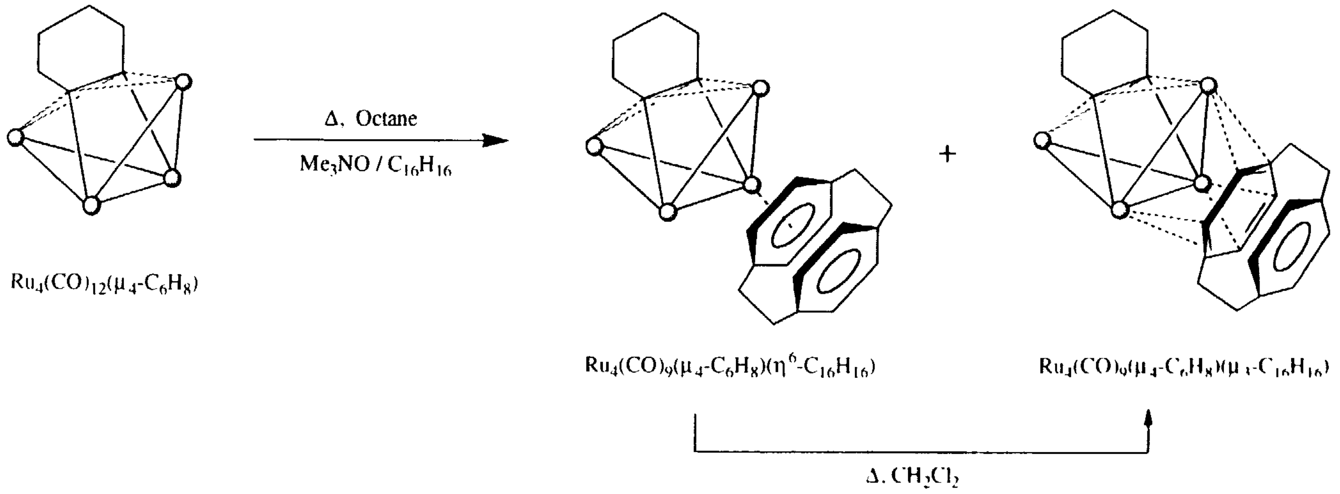

Scheme 4. Reaction of $Ru_4(CO)_{12}(\mu_4\text{-}C_6H_8)$ with [2.2]paracyclophane.

in Scheme 5. The predominant substitution takes place *pseudogeminal* to the most basic position or substituent in the already substituted ring.

There is a wealth of organic chemistry associated with [2.2]paracyclophane and its derivatives, details of which may be found in the literature [24,25]. However, studies involving the manipulation of cyclophanes whilst coordinated to transition metal centres are poorly developed in comparison. The reaction of bis(arene) ruthenium II complexes which contain one [2.2]paracyclophane ligand with nucleophiles such as H^-, CN^- or OH^-, always results in addition at the other arene [26–28]. This takes place even when the arene employed is hexamethylbenzene which is generally considered to be unreactive towards this type of reactivity. Whilst the coordinated ring of [2.2]paracyclophane would be expected to undergo nucleophilic addition, the free ring could well undergo electrophilic substitution reactions. However, as yet, work in this area has not been reported.

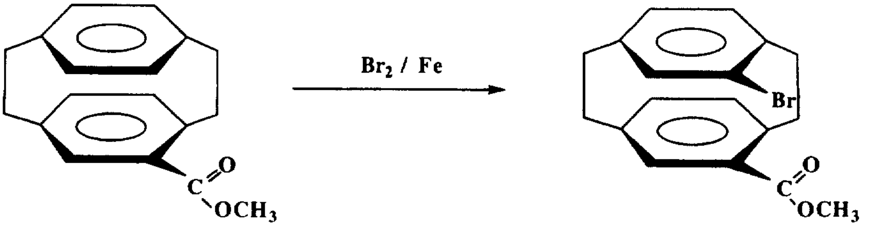

Scheme 5.

3.2. Chemical degradative decarbonylation reactions of clusters

Treatment of $Ru_3(CO)_9(\mu_3\text{-}C_{16}H_{16})$ with Me_3NO in dichloromethane only results in the formation of a dinuclear species, $Ru_2(CO)_6(\mu\text{-}C_{16}H_{16})$, as a result of cluster degradation (Scheme 6) [13]. Trimethylamine *N*-oxide has been used extensively as an oxidative decarbonylation reagent (removing CO as CO_2) in combination with a coordinating solvent, typically acetonitrile, or in a coordinatively inert solvent containing a suitable ligand. However, in this reaction it has been found that Me_3NO may bring about cluster degradation when reacted in a non-coordinating solvent. Presumably the loss of a substantial number of CO groups from the cluster results in the formation of an unstable, unsaturated cluster unit which leads to the breakdown of the cluster.

The hexanuclear cluster $Ru_6C(CO)_{14}(\mu_3\text{-}C_{16}H_{16})$ also reacts in this manner when treated with an excess of Me_3NO in dichloromethane, affording the trinuclear cluster $Ru_3(CO)_9(\mu_3\text{-}C_{16}H_{16})$ in modest yield.

3.3. Reactivity of clusters towards phosphines

The substitution chemistry of $Ru_3(CO)_9(\mu_3\text{-}C_{16}H_{16})$ [13] and $Ru_6C(CO)_{14}(\mu_3\text{-}C_{16}H_{16})$ [29] with phosphines has been examined. Both clusters readily undergo

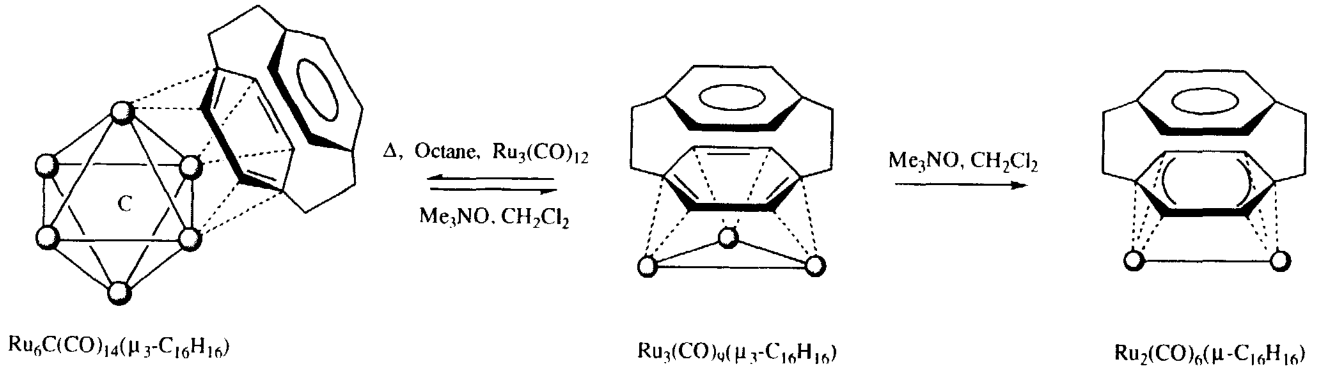

Scheme 6. Reactions involving a change in nuclearity.

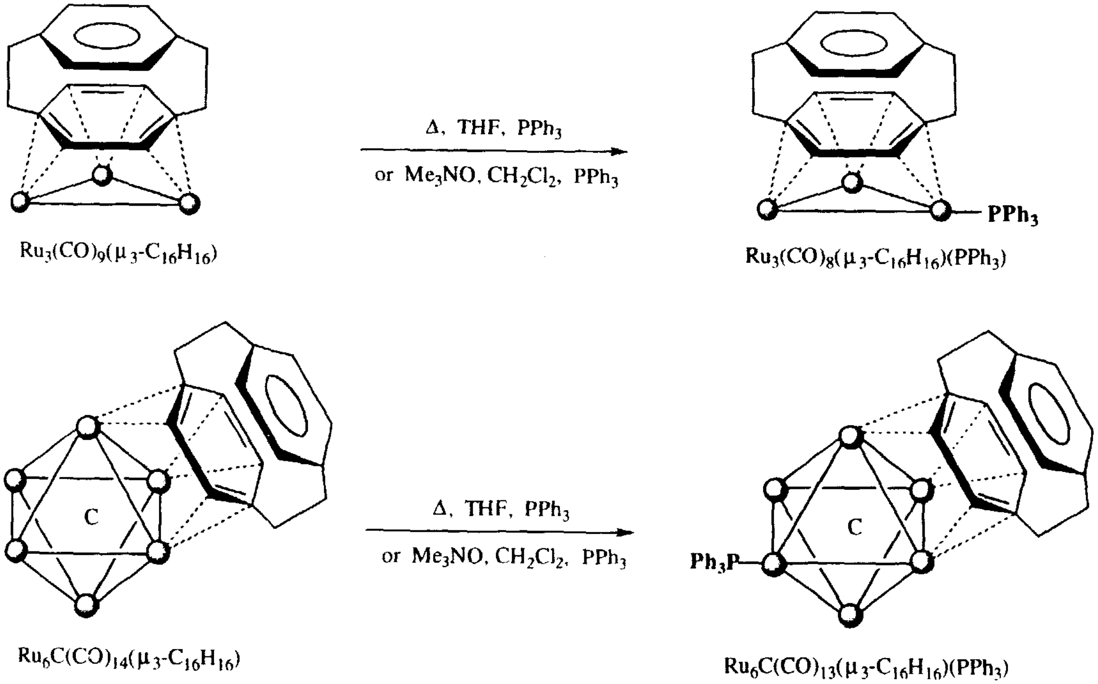

Scheme 7. Reaction of $Ru_3(CO)_9(\mu_3\text{-}C_{16}H_{16})$ and $Ru_6C(CO)_{14}(\mu_3\text{-}C_{16}H_{16})$ with triphenylphosphine.

substitution reactions in which one carbonyl group is replaced by a phosphine ligand (Scheme 7). This may be achieved either by using Me_3NO or by thermolysis in tetrahydrofuran.

3.4. Reactivity of clusters towards acetylenes

Reaction of $Ru_3(CO)_9(\mu_3\text{-}C_{16}H_{16})$ with diphenylacetylene results in the formation of three products [13]. The major product is $Ru_3(CO)_7(\mu_3\text{-}C_2Ph_2)(\eta^6\text{-}C_{16}H_{16})$ in which the cyclophane has migrated from the face-capping position to a terminal Ru atom, with the alkyne adopting a facial site. This reaction can be initiated by either thermal or chemical activation, i.e. by heating the cluster in dichloromethane under reflux in the presence of diphenylacetylene, or by treatment with two molecular equivalents of Me_3NO in the presence of diphenylacetylene at −78°C. In the thermal reaction two additional products, namely $Ru_3(CO)_7(\mu_3\text{-}\eta^2\text{-}PhC_2PhCO)(\eta^6\text{-}C_{16}H_{16})$ and $Ru_2(CO)_6(\{\mu\text{-}\eta^1{:}\eta^2\text{-}C_2Ph_2\}_2\text{-}CO)$ have also been isolated (Scheme 8). The relative yields of the three compounds obtained depend on the reaction time, with the diruthenium complex formed in highest yield as time is increased.

The alkyne cluster $Ru_6C(CO)_{12}(\mu_3\text{-}C_2Me_2)(\mu_3\text{-}C_{16}H_{16})$ may be prepared from the reaction of $Ru_6C(CO)_{14}(\mu_3\text{-}C_{16}H_{16})$ with Me_3NO in the presence of but-2-yne [30]. In this case, the cyclophane moiety maintains its facial position, with the alkyne bonding to the opposite face.

3.5. Reactivity of clusters towards cyclohexa-1,3-diene

The clusters $Ru_3(CO)_9(\mu_3\text{-}C_{16}H_{16})$ [22] and $Ru_6C(CO)_{14}(\mu_3\text{-}C_{16}H_{16})$ [16] have also been treated with Me_3NO in the presence of cyclohexa-1,3-diene, resulting in the formation of the tetranuclear cluster $Ru_4(CO)_9(\eta^4\text{-}C_6H_8)(\mu_3\text{-}C_{16}H_{16})$ and $Ru_6C(CO)_{12}(\mu\text{-}C_6H_8)(\mu_3\text{-}C_{16}H_{16})$, respectively (Scheme 9). While the formation of the latter is readily rationalised by the substitution of two CO ligands by the cyclohexa-1,3-diene moiety, the reaction in which the tetranuclear cluster is obtained from the triruthenium starting material is less straightforward. In Section 3.2 we described how the reaction of $Ru_3(CO)_9(\mu_3\text{-}C_{16}H_{16})$ with Me_3NO only led to the degradative decarbonylation of the cluster and the formation of a dinuclear product. Therefore fragmentation is not unexpected, however, in this case, it is followed by recombination with the formation of the tetrahedral cluster.

3.6. Site exchange

There are several examples in arene carbonyl clusters of ruthenium and osmium where the arene ligand undergoes migration, either reversibly or irreversibly, from a facial to a terminal site or vice versa [12], or even from one η^6 site to another (as in the square pyramidal cluster $Ru_5C(CO)_{12}(C_6H_6)$ where the benzene apparently migrates from the apical η^6 position to an η^6 site on a basal ruthenium atom) [31]. These migrations may be initiated by thermal, photochemical or chemical means, and although the precise mechanisms by which these isomerisations occur has not

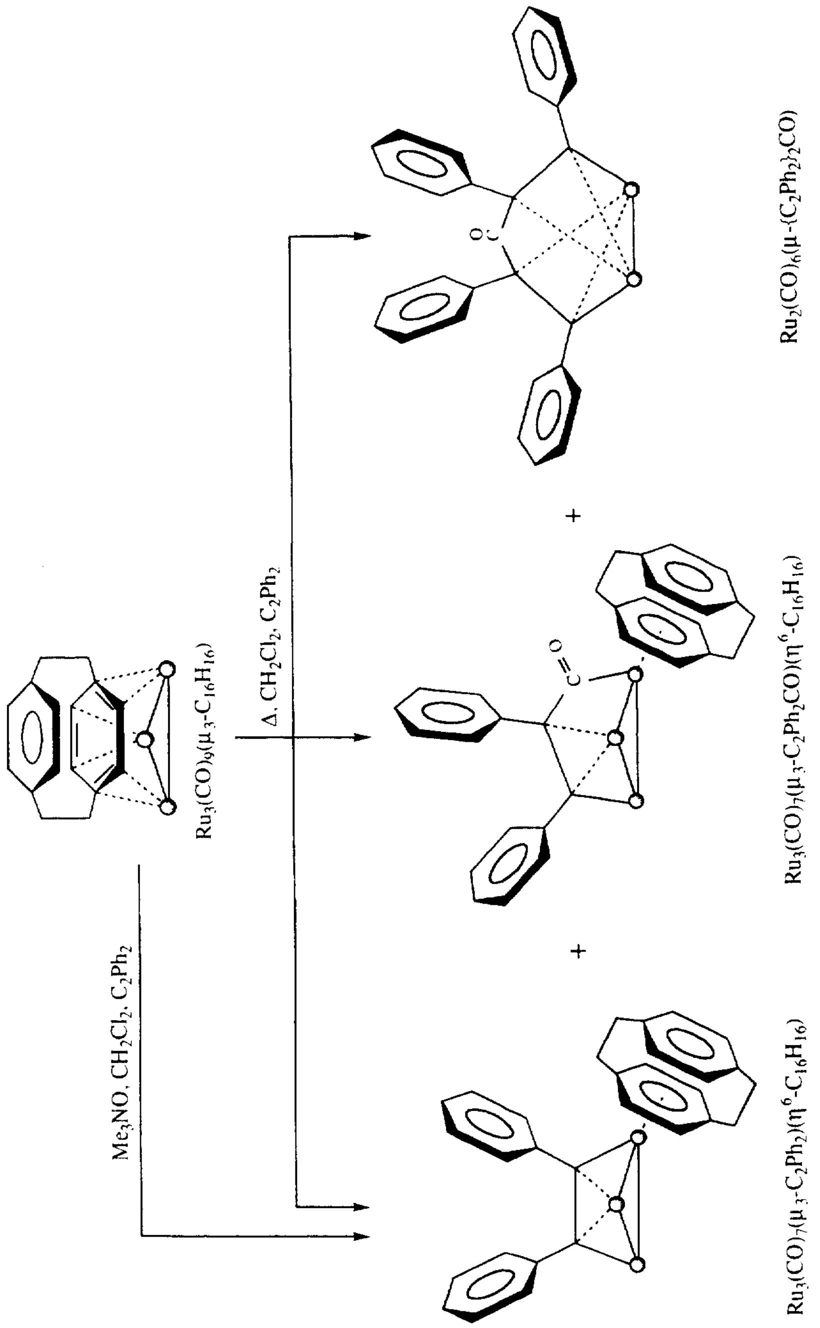

Scheme 8. Reactions of $Ru_3(CO)_9(\mu_3-C_{16}H_{16})$ with diphenylacetylene.

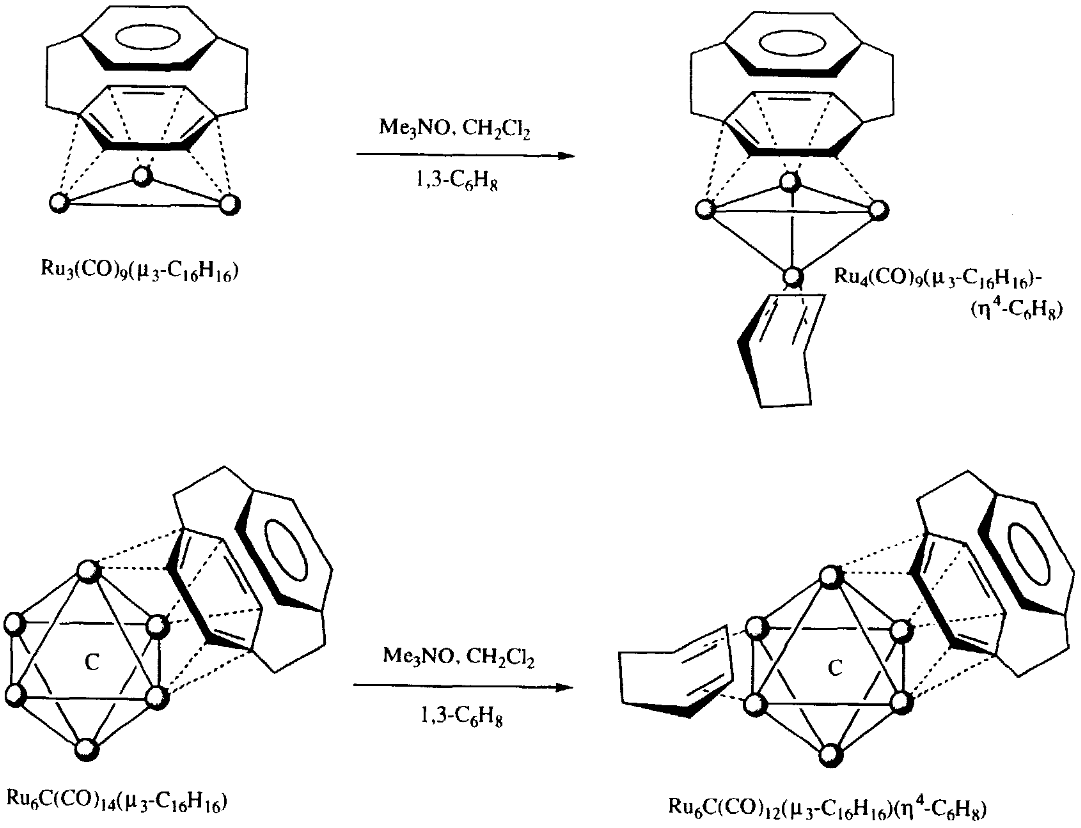

Scheme 9. Reaction of $Ru_3(CO)_9(\mu_3\text{-}C_{16}H_{16})$ and $Ru_6C(CO)_{14}(\mu_3\text{-}C_{16}H_{16})$ with cyclohexa-1,3-diene.

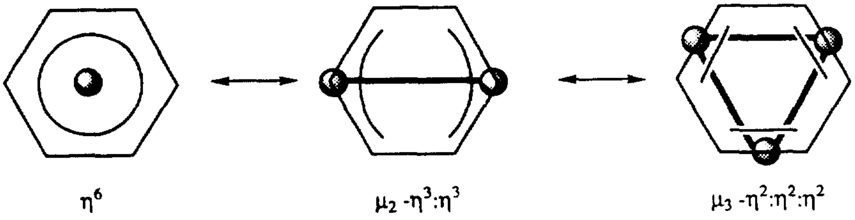

Scheme 10. The proposed migration of benzene on a cluster surface from a terminal site to a face-capping position and vice versa, via an edge-bridging intermediate.

been established, kinetic analyses have confirmed, in the case of $Ru_5C(CO)_{12}(C_6H_6)$, that the process is non-dissociative and takes place via an intramolecular mechanism [32]. From the energies involved, it is most likely that these migrations occur via arene slippage from a terminal η^6 position onto a M–M edge and then either across onto a trimetallic face or onto an alternative single metal atom. Such migrations also require a simultaneous and concerted movement of the carbonyl ligands in the opposite direction. As yet a reaction transition state or intermediate in these isomerisations has not been observed, however, a μ-η^3:η^3 type interaction between the arene and a M–M edge of the cluster seems plausible. To date, the edge-bridged bis(allyl) type bonding mode has not been observed in a cluster complex, however, the isolation of $Ru_2(CO)_6(\mu\text{-}C_{16}H_{16})$ provides an excellent model for this proposed migratory intermediate (Scheme 10) [13].

The thermolysis reaction between the butterfly cluster, $Ru_4(CO)_{12}(\mu_4\text{-}C_6H_8)$, and [2.2]paracyclophane yields $Ru_4(CO)_9(\mu_4\text{-}C_6H_8)(\eta^6\text{-}C_{16}H_{16})$ as a kinetic product which undergoes isomerisation via migration of the [2.2]paracyclophane ligand to a facial position affording $Ru_4(CO)_9(\mu_4\text{-}C_6H_8)(\mu_3\text{-}C_{16}H_{16})$ [22]. This process has not been found to be reversible. The hexanuclear cluster $Ru_6C(CO)_{14}(\mu_3\text{-}C_{16}H_{16})$ may also be prepared from the reaction between $[Ru_5C(CO)_{14}]^{2-}$ and the mononuclear complex $Ru(\eta^6\text{-}C_{16}H_{16})(MeCN)_3]^{2+}$ which again suggests the greater stability of a facial bonding site over a terminal one as the ring clearly undergoes migration in this process, and is not shown to be reversible (Scheme 11) [33].

4. Structure

4.1. The structure of [2.2]paracyclophane

The crystal structure of [2.2]paracyclophane has been determined on several occasions with significant variance between the results [34,35]. It was generally considered that the observed differences arose from the poor quality of the data accessible from the early analyses. More recent studies have led to the definitive molecular structure and have enabled an analysis of the observed thermal motion [36]. This study shows that the benzene rings are not eclipsed but equilibrate between two structures in which they are slightly staggered.

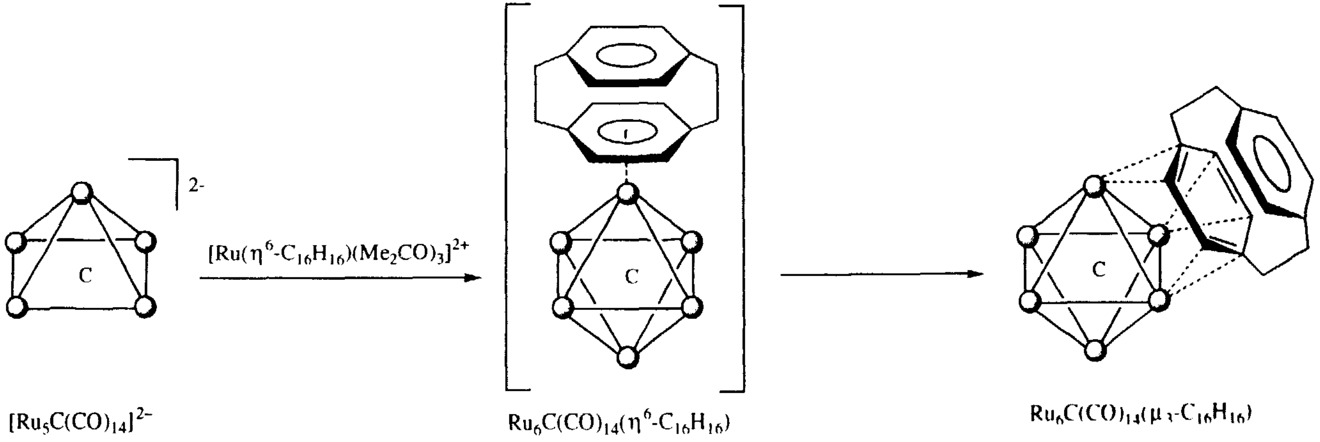

Scheme 11. Reaction of $[Ru_5C(CO)_{14}]^{2-}$ with $[Ru(\eta^6\text{-}C_{16}H_{16})(MeCN)_3]^{2+}$.

A schematic representation of [2.2]paracyclophane is shown in Fig. 3. The most noteworthy features consist of the bent rings which adopt boat-shaped conformations, the elongation of the central C–C bonds in the ethano bridges linking the rings, and the unusual bond angles between the two rings. The distance between the rings is very short (3.09 Å) and together these structural abnormalities give rise to the unique chemical properties of the molecule.

4.2. $Cr(CO)_3(\eta^6\text{-}C_{16}H_{16})$ *and related complexes: paracyclophane in the* η^6 *coordination mode*

The first solid-state structure of a cyclophane complex was established for the chromium complex $Cr(CO)_3(\eta^6\text{-}C_{16}H_{16})$ [8]. Prior to this work, it had been argued that the distance between the two parallel rings arose from a combination of two opposite effects. Firstly, the strain imposed on the bridging CH_2–CH_2 units, and secondly, the π-electron repulsion between the rings. This study showed that the distance between the two arene rings was reduced when one of the rings was coordinated to a $Cr(CO)_3$ unit. This is because the $Cr(CO)_3$ unit is a good π-acceptor and lowers the π-repulsion term described above. For the chromiumtricarbonyl complex and the clusters described herein with η^6 bonded ligands, the geometry of the benzene rings remains relatively unperturbed relative to that of the free ligand, except for the aforementioned reduction in the gap between the two rings described above.

4.3. *Edge-bridging bonding*

[2.2]Paracyclophane has been observed to bond in $\mu_2\text{-}\eta^3{:}\eta^3$ edge-bridging mode in the binuclear complex $Ru_2(CO)_6(\mu_2\text{-}\eta^3{:}\eta^3\text{-}C_{16}H_{16})$ (Fig. 4) [13]. The paracyclophane ligand bridges the two metal centres, with each ruthenium atom interacting with three carbon atoms of the bonded ring. A close examination of this $\mu\text{-}\eta^3{:}\eta^3$ interaction reveals that the coordinated ring adopts a more pronounced boat conformation with an angle between the two η^3-enyl planes of 56°. This is markedly different from the corresponding dihedral angle found in free [2.2]paracyclophane, in this case the angle between the two enyl planes is only 23°. These observations indicate that significant deviations from planarity, and hence

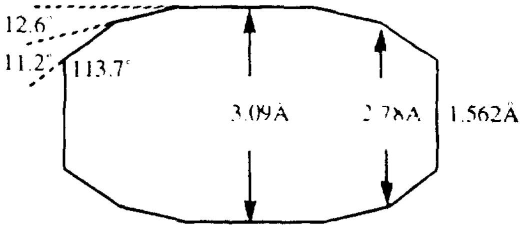

Fig. 3. The key structural features of [2.2]paracyclophane.

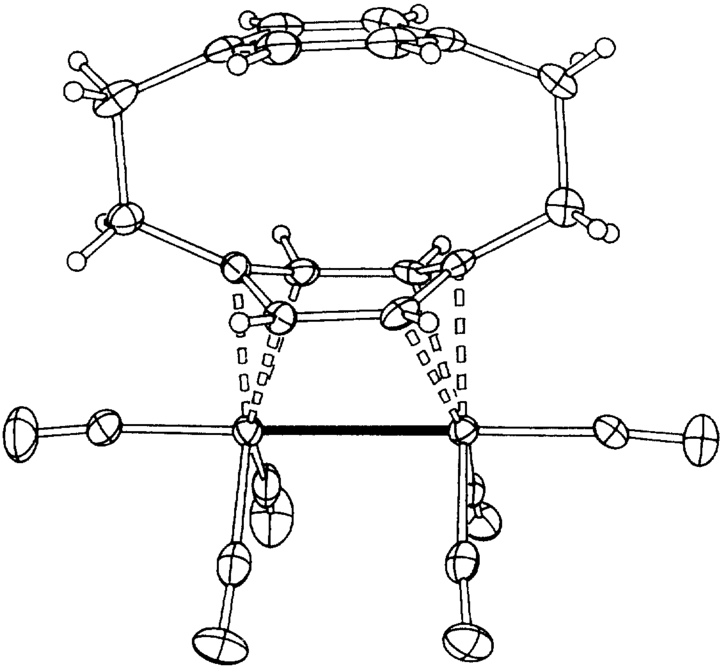

Fig. 4. The molecular structure of $Ru_2(CO)_6(\mu_2\text{-}\eta^3{:}\eta^3\text{-}C_{16}H_{16})$.

different hybridisation states of the ring C atoms, are essential for an efficient overlap between the metal and ligand orbitals, and a stable $\eta^3{:}\eta^3$ interaction between the organic ring and the two metal atoms. In this connection it is also worth noting that the mean C–C bond lengths of the enyl sections of the ring are shorter than the C–C bonds linking the two enyl units (mean 1.41(1) vs. 1.48(1) Å, respectively). A similar bonding mode has also been observed for benzene in the dirhodium complex $Rh_2(Cp)_2(\mu_2\text{-}\eta^3{:}\eta^3\text{-}C_6H_6)$, which also exhibits deviations from planarity towards a boat-shaped conformation [37].

The distortions described above for the coordinated cyclophane ring are not observed in the unattached ring but are actually slightly reversed. The angle between the two enyl planes of 18° is less than in the free ligand itself. The bridgehead carbon atoms of the coordinated ring lie almost directly above the two ruthenium atoms, and their Ru–C distances of 2.187(7) and 2.191(7) Å, respectively are notably shorter than the remaining four bonds (mean 2.273(7) Å).

4.4. *Facial bonding*

There are numerous examples of μ_3 face-capping [2.2]paracyclophane ligands, in fact it appears to be the preferred bonding mode in clusters [13–16,22]. The same general modifications to the ring are present in all the known structures. The general features of the [2.2]paracyclophane ligand in the μ_3 coordination mode can be illustrated with reference to the molecular structure of $Ru_3(CO)_8(PPh_3)(\mu_3\text{-}\eta^2\text{:}\eta^2\text{:}\eta^2\text{-}C_{16}H_{16})$ as determined by single crystal X-ray diffraction (Fig. 5) [13]. The coordinated ring is flattened in comparison to the free ligand, the angle between the boat ends is 16° (cf. free PCP, 23°) [7]. The unattached ring is essentially unchanged with an angle between the enyl planes of 24°. The gap between the rings is also reduced, as is the case in all of the complexed ligands.

An alternative face-capping configuration has been observed in $Ru_4(CO)_9(\eta^4\text{-}C_6H_8)(\mu_3\text{-}C_{16}H_{16})$ [22]. A view of the C_6 ring interaction with the underlying Ru_3 triangle is shown in Fig. 6. The bonding is related to that observed in the facially bound cyclohexadienyl ring found in $HM_3(CO)_9(\mu_3\text{-}\eta^1\text{:}\eta^2\text{:}\eta^2\text{-}C_6H_7)$ (M = Ru or Os) [38]. In $Ru_4(CO)_9(\eta^4\text{-}C_6H_8)(\mu_3\text{-}C_{16}H_{16})$ the ring bonds via one η^1 bond [2.115(9) Å] and two η^2 interactions which consist of one long [mean 2.480(9) Å] and one short [mean 2.184(8) Å] bond. The angle between the planes of the central rectangle and the triangular ends is 1 and 17° (cf. 13° for the comparable angle in the free molecule) [13]. This $\eta^1\text{:}\eta^2\text{:}\eta^2$ bonding mode is usually associated with a five-electron donor, however, NMR studies in solution indicate that the ligand is symmetrical and rotates freely, thus the unusual bonding pattern is considered to be due to solid-state packing effect.

In $Ru_6C(CO)_{15}(\mu_3\text{-}C_{16}H_{16}\text{-}\mu_2\text{-}O)$ the C_6 ring exhibits an $\eta^1\text{:}\eta^2\text{:}\eta^2$ bonding mode similar to that in the previous example except that one carbon forms a σ-bond with an oxygen atom (Fig. 7) [14]. In this case the bonded ring contributes five electrons towards cluster bonding.

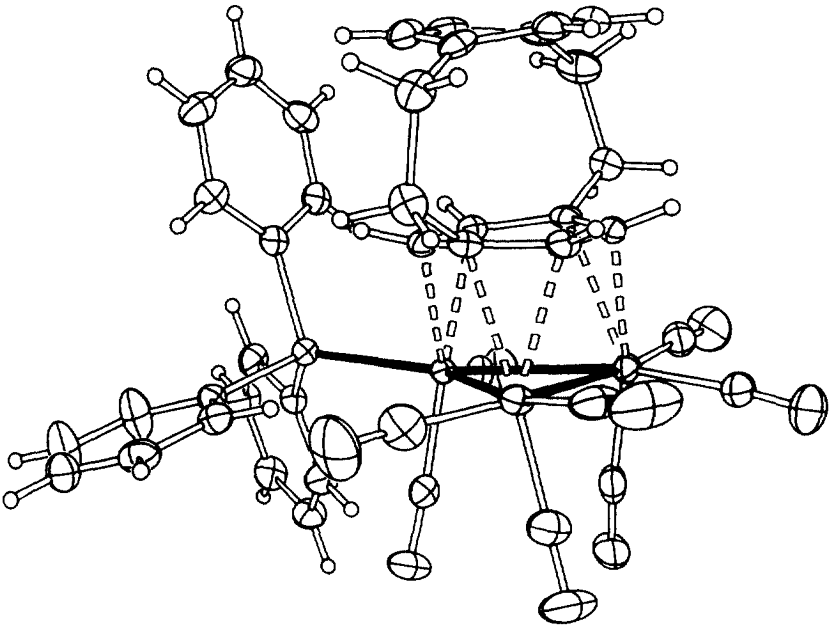

Fig. 5. The key structural features of [2.2]paracyclophane when bonded over a trimetal face in $Ru_3(CO)_8(\mu_3\text{-}C_{16}H_{10})(PPh_3)$.

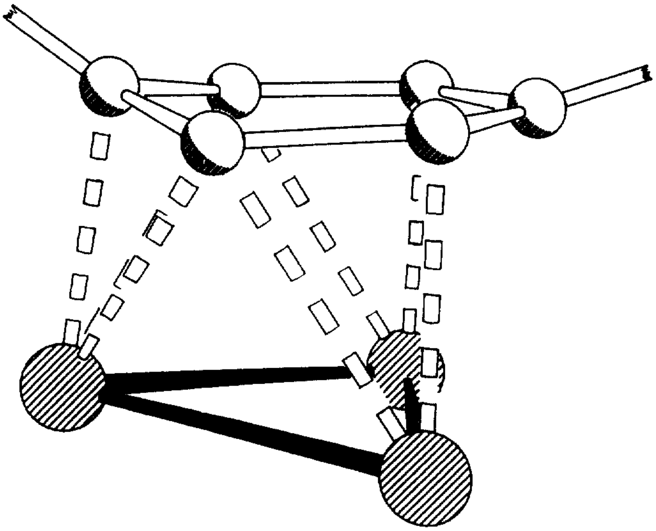

Fig. 6. View of the metal–ring interaction in $Ru_4(CO)_9(\eta^4\text{-}C_6H_8)(\mu_3\text{-}C_{16}H_{16})$.

4.5. Comparisons of conformational variations

When [2.2]paracyclophane is bonded to a triangular metal face the C_6 ring may adopt different degrees of torsion with respect to the underlying Ru_3 framework (Fig. 8) [16]. In most of these clusters the midpoints of the C=C bonds tend to eclipse the ruthenium atoms, which is typical for benzene when μ_3 bonded, and this orientation of the ring is observed in $Ru_6C(CO)_{11}(\mu_3\text{-}C_{16}H_{16})(\eta^6\text{-}C_{16}H_{16})$. However, in $Ru_6C(CO)_{14}(\mu_3\text{-}C_{16}H_{16})$ and $Ru_6C(CO)_{12}(\mu\text{-}C_6H_8)(\mu_3\text{-}C_{16}H_{16})$ the rings are rotated slightly and approach a situation where the C=C bonds lie nearly parallel to the Ru–Ru bonds of the trimetal face. This is reflected in the value of the Ru–C distances which alternate in their mean length, the difference increasing in the order $Ru_6C(CO)_{11}(\mu_3\text{-}C_{16}H_{16})(\eta^6\text{-}C_{16}H_{16})$ [2.23(2) versus 2.34(2) Å ($\Delta = 0.11$)] < $Ru_6C(CO)_{14}(\mu_3\text{-}C_{16}H_{16})$ [2.20(1) versus 2.37(1) Å ($\Delta = 0.17$)] < $Ru_6C(CO)_{12}(\mu\text{-}C_6H_8)(\mu_3\text{-}C_{16}H_{16})$ [2.17(2) versus 2.45(2) Å ($\Delta = 0.28$)]. The fact that, on going from $Ru_6C(CO)_{11}(\mu_3\text{-}C_{16}H_{16})(\eta^6\text{-}C_{16}H_{16})$ to $Ru_6C(CO)_{14}(\mu_3\text{-}C_{16}H_{16})$ and then to $Ru_6C(CO)_{12}(\mu\text{-}C_6H_8)(\mu_3\text{-}C_{16}H_{16})$, the ‘short’ Ru–C bond distances become progressively shorter, while the ‘long’ Ru–C parameters increase, clearly indicates that the separation between the ring and the metal triangle planes is retained while the ligand moves from a near-staggered towards a near-eclipsing of the C atoms over the Ru atoms.

4.6. Clusters

The majority of cluster–cyclophane complexes have metal frameworks which are familiar to the cluster chemist, viz. triangular, tetrahedral, butterfly, octahedral and bicapped octahedral. For this reason they will not be discussed and only clusters with more unusual skeletal frameworks will be described.

The structure of the hexanuclear cluster $Ru_6C(CO)_{15}(\mu_3\text{-}C_{16}H_{16}\text{-}\mu_2\text{-}O)$ is illustrated in Fig. 9 [14]. It has an unusual metal framework with three metal–metal contacts, less than that present in an octahedron. One of the open edges is spanned by a bridging O atom which contributes three electrons to the cluster framework, leaving one 'unused' lone-pair, thereby giving a total valance electron count of 90. The interstitial carbido atom sits in the middle of a bridged butterfly subsystem defined by Ru(1) and Ru(6) (wing-tip atoms) and Ru(2) and Ru(4) (hinge atoms); the wing-tips being bridged by Ru(5). The distances between the carbido atom and the wing-tip ruthenium atoms [1.94(2), 1.97(2) Å] are shorter than those from the bridging atom [Ru(5)–C 2.04(2) Å], and from the hinge atoms [2.09(2) and 2.17(2) Å]. Ru(3) is too far from the interstitial carbido atom to interact [Ru(3)–C 3.11 Å].

The solid-state structures of two octaruthenium clusters, $Ru_8(\mu\text{-}H)_2(\mu_6\text{-}\eta^2\text{-}CO)(CO)_{19}(\eta^6\text{-}C_{16}H_{16})$ and $Ru_8(\mu_6\text{-}\eta^2\text{-}CO)(\mu_4\text{-}\eta^2\text{-}CO)(CO)_{18}(\eta^6\text{-}C_{16}H_{16})$, are shown in Figs. 10 and 11, respectively [18]. Their metal frameworks consists of an 'open' array of the eight ruthenium atoms comprising a square-based pyramid in which two adjacent basal edges are bridged by two ruthenium atoms, these are fused and this edge is itself bridged by a ruthenium atom. The cyclophane ligand is η^6 bound to the only basal vertex of the square pyramid not involved in edge bridging. In each cluster a *dihapto* carbonyl ligand sits in an almost 'interstitial' cavity where it

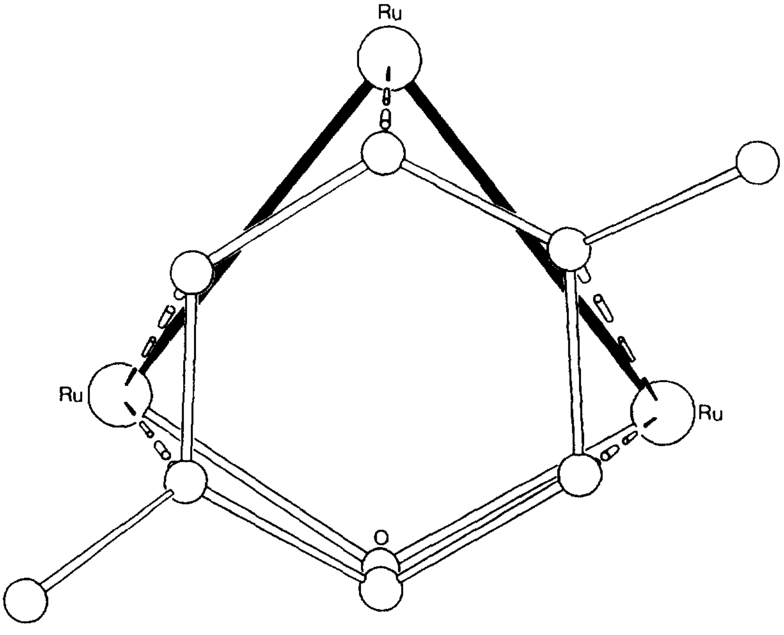

Fig. 7. Projection of the bound paracyclophane ring over the Ru_3 face in $Ru_6C(CO)_{15}(\mu_3\text{-}C_{16}H_{16}\text{-}\mu_2\text{-}O)$.

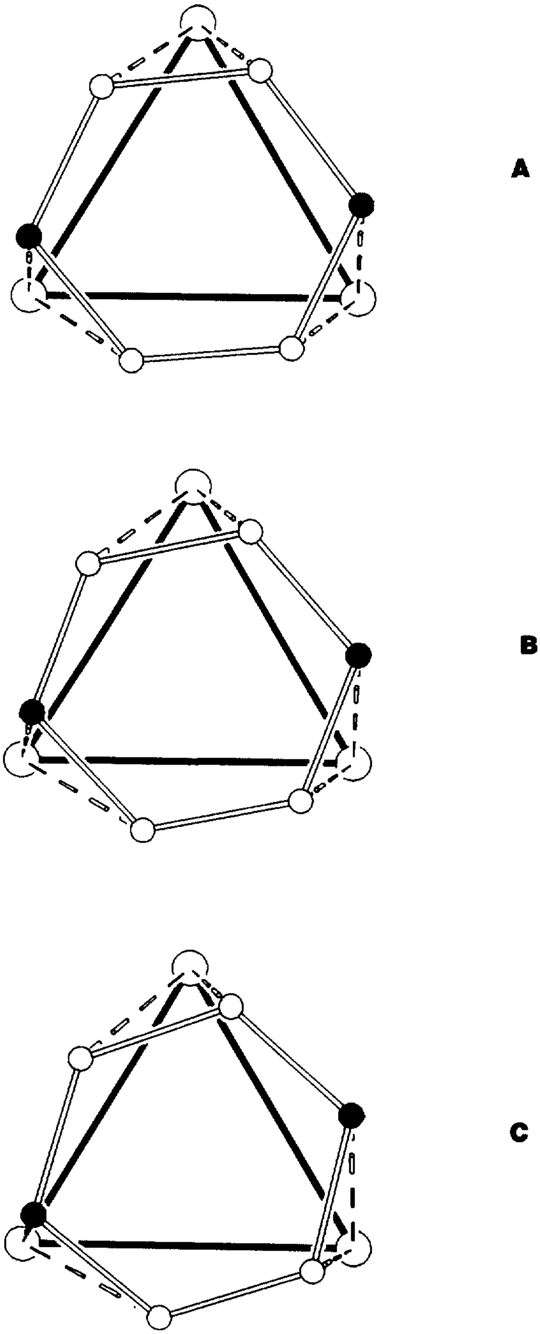

Fig. 8. Projection of the bound paracyclophane ring over the trimetal face in: (A) $Ru_6C(CO)_{11}(\mu_3\text{-}C_{16}H_{16})(\eta^6\text{-}C_{16}H_{16})$; (B) $Ru_6C(CO)_{14}(\mu_3\text{-}C_{16}H_{16})$ and (C) $Ru_6C(CO)_{12}(\mu_3\text{-}C_{16}H_{16})(\eta^4\text{-}C_6H_8)$.

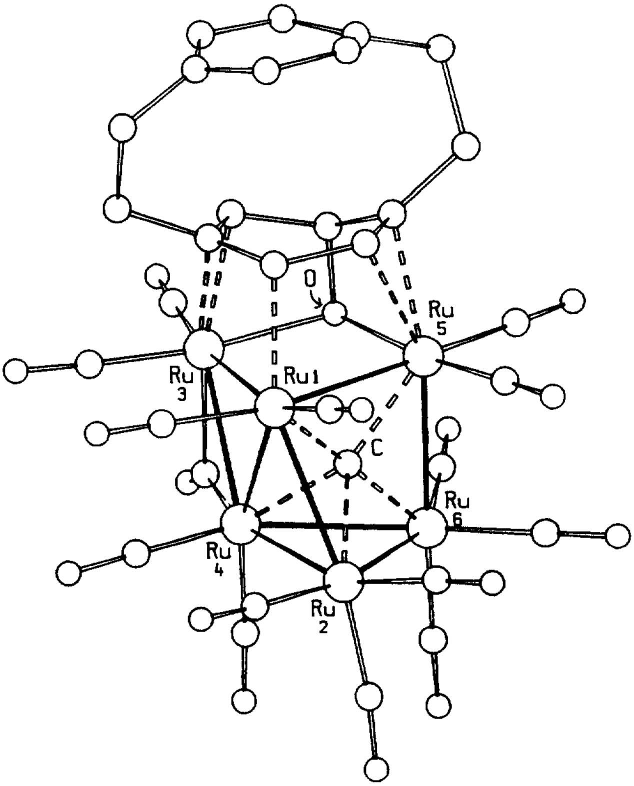

Fig. 9. The solid-state molecular structure of $Ru_6C(CO)_{15}(\mu_3\text{-}C_{16}H_{16}\text{-}\mu_2\text{-}O)$.

bridges six metal atoms; the carbon coordinating to the four square pyramidal basal ruthenium atoms, and the oxygen to the two fused edge-bridging ruthenium atoms. The C–O ligand acts as a six-electron donor, and it appears that these compounds provide the first examples of a carbonyl coordinated in $\mu_6\text{-}\eta^2$ fashion. The bond length of this bridging C–O is 1.378(11) Å in $Ru_8(\mu\text{-H})_2(\mu_6\text{-}\eta^2\text{-}CO)(CO)_{19}(\eta^6\text{-}C_{16}H_{16})$ and only slightly shorter in the other cluster [1.355(6) Å]. In this latter compound there is a second *dihapto* CO which bonds over a Ru_4 butterfly site. Although not as long as the $\mu_6\text{-}\eta^2$ CO bond length the $\mu_4\text{-}\eta^2$ C–O bond length is still longer than terminal CO ligands [1.139(7) Å].

5. Mass spectrometry

One of our objectives has been to prepare oligomers and polymers containing cluster units. Such species have been prepared with the coinage metals [39], however, with clusters, using conventional synthetic techniques, it has not even been possible, as yet, to attach a cluster to both rings of the same [2.2]paracyclophane moiety.

In recent studies investigating the potential of UV laser desorption mass spectrometry as a method of obtaining accurate mass ions of arene clusters, peaks corresponding to the formation of oligomers have been produced [40]. The negative ion mass spectrum obtained for $Ru_6C(CO)_{14}(\mu_3\text{-}C_{16}H_{16})$ is shown in Fig. 12. The parent cluster region does not give a peak for the unfragmented cluster ($m/z = 1218$), but peaks are observed which correspond to successive loss of CO from the parent cluster (at $m/z = 1191$, 1163, 1135, etc.). There is no evidence for the loss of the [2.2]paracyclophane ligand in the desorption process. Above this grouping of peaks, higher mass ion peaks, corresponding to the products of gas-phase aggregation, are observed with diminishing intensity up to m/z values of 5000. The weight of the additive unit corresponds to the formula $Ru_6C(CO)_{14-x}(C_{16}H_{16})$ ($x = 3$–6) and experiments are in hand to delineate the aggregative process. We have also found that $Cr(C_{16}H_{16})(CO)_3$ undergoes complete CO loss in the UV laser desorption mass spectrometer [41]. The resulting unsaturated $Cr(C_{16}H_{16})$ fragments are highly reactive and undergo condensation to form oligomers containing up to seven chromium–cyclophane units.

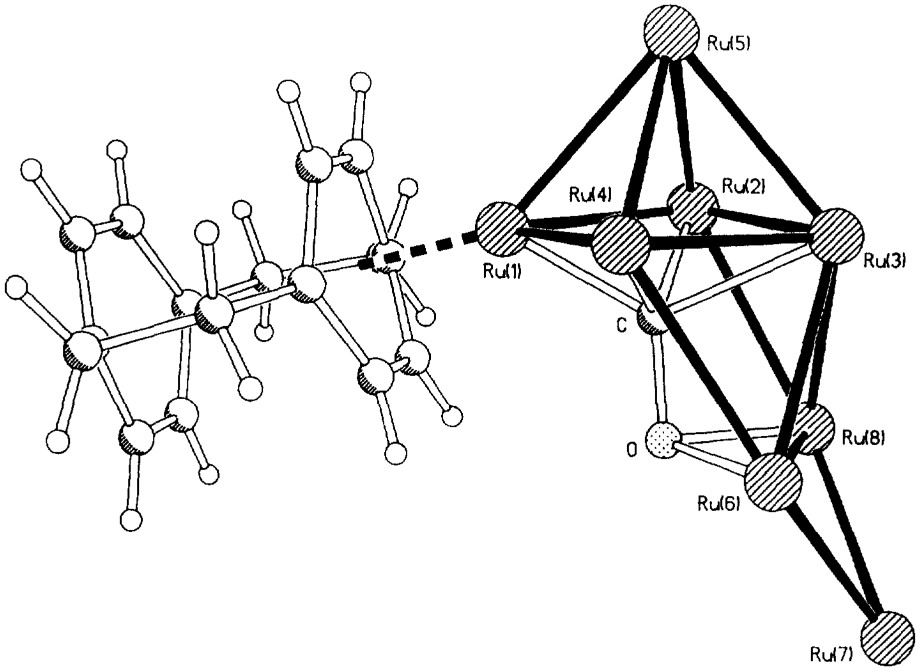

Fig. 10. The solid-state molecular structure of $Ru_8(\mu\text{-}H)_2(\mu_6\text{-}\eta^2\text{-}CO)(CO)_{19}(\eta^6\text{-}C_{16}H_{16})$. The terminal COs have been omitted for clarity.

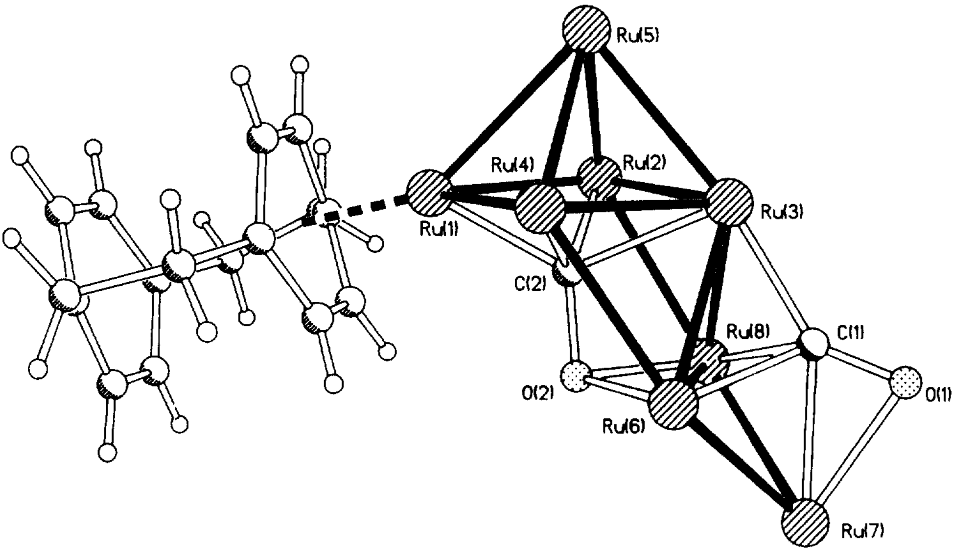

Fig. 11. The solid-state molecular structure of $Ru_8(\mu_6\text{-}\eta^2\text{-}CO)(\mu_4\text{-}\eta^2\text{-}CO)(CO)_{18}(\eta^6\text{-}C_{16}H_{16})$. The terminal COs have been omitted for clarity.

6. NMR spectroscopy

The aromatic protons of the complexed benzene deck in a [2.2]paracyclophane complex are shifted to lower frequency. This effect is similar to the upfield shifts observed for the aromatic protons of simple arenes when complexed with transition metals [42]. The change in frequency of these protons during complexation is undoubtedly a combination of effects such as a rehybridisation of the bound aromatic ring carbons, a loss of ring current, the direct effect of the magnetic anisotropy of the metal atoms, and changes in electron density. It is apparent, however, that upon complexation the aromatic protons of the unbound cyclophane deck also change, this time to higher frequency. The distance of these protons from the metal is sufficiently great that direct metal anisotropy effects from the metal are negligible, and the most significant effect causing this downfield shift involves a loss of ring current in the bound aromatic ring, which causes a decrease in shielding on the opposite deck.

The ^{1}H-NMR chemical shift values (for the ring protons only) of several cyclophane–cluster complexes are shown in Table 1, together with the value of the free ligand. From this table several trends can be noted. The difference in chemical shift between the protons of the free and coordinated rings is greater in clusters than in mononuclear complexes and also larger when the cyclophane is facially bound than when bonded η^6 to a cluster. This phenomenon is also exhibited in benzene clusters and is thought to arise because the interaction with three metal atoms of a cluster face causes a greater reduction in ring current, a greater rehybridisation of the bound ring, and also a greater direct effect on the cyclophane from the magnetic anisotropy of the metals. For a particular bonding type, namely the face-capping coordination mode, the difference in chemical shift (the difference in shift between the unattached and coordinated ring protons of [2.2]paracyclophane) varies as a function of cluster size and, although caution should be exercised in any correlation of this type, these changes in shift probably reflect the change in electron withdrawing ability of the cluster surface as the nuclearity of the cluster is increased [29]. The large shielding effect experienced by the complexed cyclophane ring appears to be a general phenomenon observed in both the ^{1}H- and ^{13}C-NMR spectra of any classical, cyclic, aromatic system in which all ring carbons are involved in π-bonding to a metal [43]. Increased shielding is experienced as the nuclearity of the cluster is increased, presumably due to the additional electron withdrawing ability of the cluster as it increases in size. Hence, a comparison of the ^{1}H-NMR spectra of the phosphine complexes with those of the parent compounds is worth considering, as replacement of carbonyl ligands on a cluster by

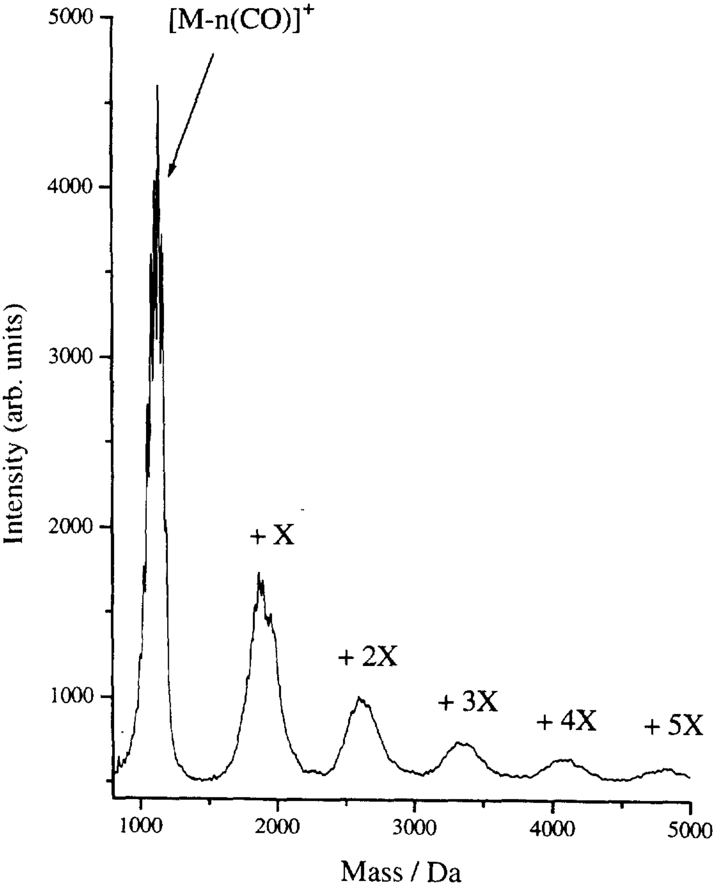

Fig. 12. The laser desorption mass spectrum of $Ru_6C(CO)_{14}(\mu_3\text{-}C_{16}H_{16})$ (X = cluster aggregate unit).

Table 1
^{1}H-NMR values (ppm) of some [2.2]paracyclophane–ruthenium cluster compounds. The values for the free ligand are reported for comparison

	Free ring δ	Bound ring δ	Δ
[2.2]paracyclophane–$C_{16}H_{16}$	6.47	—	—
$Ru_3(CO)_9(\mu_3\text{-}C_{16}H_{16})$	7.22	3.76	3.46
$Ru_3(CO)_8(PPh_3)(\mu_3\text{-}C_{16}H_{16})$	7.32	3.12	4.20
$Ru_6C(CO)_{14}(\mu_3\text{-}C_{16}H_{16})$	7.44	3.40	4.04
$Ru_6C(CO)_{13}(PPh_3)(\mu_3\text{-}C_{16}H_{16})$	7.43	3.38	4.05
$Ru_6C(CO)_{13}(PCy_3)(\mu_3\text{-}C_{16}H_{16})$	7.36	3.22	4.14
$Ru_8(\mu\text{-}H)_4(CO)_{18}(\eta^6\text{-}C_{16}H_{16})$	6.78	4.51	2.27
$Ru_8(\mu\text{-}H)_2(\mu_6\text{-}CO)(CO)_{19}(\eta^6\text{-}C_{16}H_{16})$	6.89	4.40	2.49

Δ = difference in chemical shifts between the free and coordinated ring protons (ppm).

more basic phosphine ligands should increase the electron density on the central cluster unit. A comparison of the chemical shift values of the parent clusters with their phosphine derivatives shows that this trend is observed, with the addition of a phosphine generally increasing Δ and always causing a shift of the bound ring to lower frequency. This may also be compared to the triosmium benzene cluster $Os_3(CO)_9(\mu_3\text{-}C_6H_6)$, in which the chemical shift of the benzene ring protons is reduced in frequency from δ 4.42 to 3.87 ppm upon substitution of one carbonyl group for a triphenylphosphine ligand [44].

The coordination of a μ_3 arene over a trimetallic face may be described in terms of the Dewar–Chatt–Duncanson approach. Interactions of this type capitalise on both the electron density donation and acceptance by benzene frontier orbitals in a synergic fashion, and have been proposed for the μ_3 benzene ligand [44,45]. The metal-to-arene backbonding interaction is thought to play a part in the movement of the resonance to lower frequency. Firstly, an increase in π-electron density at the ring leads to substantial shielding of the carbon nuclei [46], and secondly the π-backdonation results in an increase in p-character for the ring carbons which should again lead to increased shielding of both ^{1}H and ^{13}C nuclei [47]. These factors also partially account for the differences in shielding between terminally and facially bound arenes, and changes of chemical shifts with cluster nuclearity, with the larger degree of shielding observed for the μ_3 ligand reflecting a greater π-acidity for benzene when bonded in this fashion. This effect is also apparent from infrared spectroscopic studies which indicate that ν_{C-H} modes for the terminal and face-capping ligands occur at significantly different energies [44].

Although no investigations of this type have been carried out on the [2.2]paracyclophane clusters, the principal bonding interactions are expected to be similar. Therefore, when a carbonyl is replaced by a more basic phosphine ligand the electron density associated with the cluster framework is increased. This in turn causes a stronger backbonding interaction, which results in an enhanced shielding effect and hence chemical shifts of the coordinated ring protons arise at lower frequencies. It is also apparent that the effect of the phosphine is far more noticeable, in terms of these shift values, on the trinuclear cluster than on the hexanuclear cluster, presumably since the additional electron density from the phosphine ligand is spread over three metal atoms instead of six, and also there are less carbonyl ligands present in the molecule onto which this extra electron density can be dispersed. Also, the more basic the phosphine the larger the changes in chemical shift.

7. Conclusions and outlook

The use of [2.2]paracyclophane in cluster chemistry serves a variety of purposes. Primarily, it has been used to produce facially bonded arene derivatives, not always available to the simpler arenes. They also act as probes of the electron density at the cluster surface as reflected by ^{1}H-NMR spectroscopy. Laser desorption studies have indicated that it is possible to produce cluster–cyclophane aggregates although their precise composition is unknown. However, we are currently conducting a series of experiments to help us understand these interesting phenomena more fully, as well as preparing clusters with other cyclophane ligands.

Acknowledgements

We would like to thank The Royal Society for providing P.J. Dyson with a University Research Fellowship.

References

[1] C.J. Brown, A.C. Farthing, Nature (London) 164 (1949) 915.
[2] D.J. Cram, H. Steinberg, J. Am. Chem. Soc. 73 (1951) 5691.
[3] F. Vögtle, P. Neumann, Tetrahedron 26 (1970) 5847.
[4] K. Kleinschroth, H. Hopf, Angew. Chem. Int. Ed. Engl. 21 (1982) 469.
[5] M.M. Pellegrin, Rec. Trav. Chim. Pays-Bas 18 (1899) 457.
[6] V. Boekelheide, Acc. Chem. Res. 13 (1980) 65.
[7] D.J. Cram, D.I. Wilkinson, J. Am. Chem. Soc. 82 (1960) 5721.
[8] Y. Kai, N. Yasnoka, N. Kasai, Acta Crystallogr. B 34 (1978) 2840.
[9] J. Schulz, F. Vögtle, Top. Curr. Chem. 172 (1994) 41.
[10] R. Gleiter, M. Merger, Angew. Chem. Int. Ed. Engl. 36 (1997) 2426.
[11] A. de Meijere, B. König, Synlett (1997) 1221.
[12] D. Braga, P.J. Dyson, F. Grepioni, B.F.G. Johnson, Chem. Rev. 94 (1994) 1585.
[13] A.J. Blake, P.J. Dyson, S.L. Ingham, B.F.G. Johnson, C.M. Martin, Organometallics 14 (1995) 862.
[14] P.J. Dyson, B.F.G. Johnson, C.M. Martin, D. Reed, D. Braga, F. Grepioni, J. Chem. Soc. Dalton Trans. (1995) 4113.
[15] D. Braga, F. Grepioni, E. Parisini, P.J. Dyson, A.J. Blake, B.F.G. Johnson, J. Chem. Soc. Dalton Trans. (1993) 2951.
[16] P.J. Dyson, B.F.G. Johnson, C.M. Martin, A.J. Blake, D. Braga, F. Grepioni, E. Parisini, Organometallics 13 (1994) 2113.

[17] D. Braga, F. Grepioni, P.J. Dyson, B.F.G. Johnson, C.M. Martin, J. Chem. Soc. Dalton Trans. (1995) 909.
[18] C.M. Martin, P.J. Dyson, S.L. Ingham, B.F.G. Johnson, A.J. Blake, J. Chem. Soc. Dalton Trans. (1995) 2741.
[19] P.J. Bailey, M.J. Duer, B.F.G. Johnson, J. Lewis, G. Conole, M. McPartlin, H.R. Powell, C.E. Anson, J. Organomet. Chem. 383 (1990) 441.
[20] B.F.G. Johnson, R.D. Johnston, J. Lewis, J. Chem. Soc. A (1968) 2865.
[21] H. Ohno, H. Horita, T. Otsubo, Y. Sakata, S. Misumi, Tetrahedron Lett. (1977) 265.
[22] A.J. Blake, P.J. Dyson, S.L. Ingham, B.F.G. Johnson, C.M. Martin, J. Chem. Soc. Dalton Trans. (1995) 1063.
[23] F. Vögtle, P. Newmann, Top. Curr. Chem. 48 (1974) 67.
[24] P.M. Keetin, S.M. Rosendield, Cyclophanes, vols. I and II, Academic Press, London, 1983.
[25] F. Vögtle, Cyclophane Chemistry, Wiley, Chichester, UK, 1993.
[26] S.G. Davies, M.L.H. Green, D.M.P. Mingos, Tetrahedron 34 (1978) 3047.
[27] R.T. Swann, A.W. Hanson, V. Boekelheide, J. Am. Chem. Soc. 108 (1986) 3324.
[28] M.R.J. Elsegood, J.W. Steed, D.A. Tocher, J. Chem. Soc. Dalton Trans. (1992) 1797.
[29] A.J. Blake, P.J. Dyson, S.L. Ingham, B.F.G. Johnson, C.M. Martin, Trans. Met. Chem. (1995) 557.
[30] R.L. Mallors, A.J. Blake, S. Parsons, B.F.G. Johnson, P.J. Dyson, D. Braga, F. Grepioni, E. Parisini, J. Organomet. Chem. 532 (1997) 133.
[31] D.B. Brown, P.J. Dyson, B.F.G. Johnson, D. Parker, J. Organomet. Chem. 491 (1995) 189.
[32] P.J. Dyson, B.F.G. Johnson, D. Braga, Inorg. Chim. Acta 222 (1994) 299.
[33] P.J. Dyson, unpublished results.
[34] J.J. Brown, J. Chem. Soc. (1953) 3265.
[35] K. Lonsdale, J.J. Milledge, K.V.K. Rao, Proc. R. Soc. London Ser. A 255 (1960) 82.
[36] H. Hope, J. Bernstein, K.N. Trueblood, Acta Crystallogr. B 28 (1972) 1733.
[37] J. Muller, P.E. Gaede, K. Qiao, Angew. Chem. Int. Ed. Engl. 32 (1993) 1697.
[38] D. Braga, F. Grepioni, E. Parisini, B.F.G. Johnson, C.M. Martin, J.G.M. Nairn, J. Lewis, M. Martinelli, J. Chem. Soc. Dalton Trans. (1993) 1891.
[39] U. Schmidbaur, W. Bublak, M.V. Haenal, B. Huber, G. Müller, Angew. Chem. Int. Ed. Engl. 25 (1986) 1089.
[40] M.J. Dale, P.J. Dyson, B.F.G. Johnson, C.M. Martin, P.R.R. Langridge-Smith, R. Zenobi, J. Chem. Soc. Chem. Commun. (1995) 1689.
[41] M.J. Dale, P.J. Dyson, unpublished results.
[42] M.A. Bennett, T.W. Matheson, G.B. Robertson, A.K. Smith, P.A. Tucker, Inorg. Chem. 21 (1980) 4405.
[43] V. Graves, J.J. Lagowski, J. Organomet. Chem. 120 (1976) 397.
[44] M.A. Gallop, M.P. Gomez-Sal, C.E. Housecroft, B.F.G. Johnson, J. Lewis, S.M. Owen, P.R. Raithby, A.H. Wright, J. Am. Chem. Soc. 114 (1992) 2502.
[45] D. Braga, F. Grepioni, B.F.G. Johnson, J. Lewis, C.E. Housecroft, M. Martinelli, Organometallics 10 (1991) 1260.
[46] G.A. Olah, G.D. Mateescu, J. Am. Chem. Soc. 92 (1970) 1430.
[47] B.E. Mann, B.F. Taylor, ^{13}C NMR Data for Organometallic Compounds, Academic Press, London, 1981.